Clim Dyn manuscript No.
(will be inserted by the editor)

Robustness of the simulated tropospheric response to ozone depletion

William J. M. Seviour · Darryn W. Waugh ·

Lorenzo M. Polvani · Gustavo J. P. Correa

Received: date / Accepted: date

Abstract Recent modeling studies have differed as to the magnitude of the response of the Southern Hemisphere tropospheric circulation to ozone depletion. This inconsistency may be a result of different model dynamics, different ozone forcing, or differences in the analysis. Here the summertime tropospheric response is analyzed across a hierarchy of climate

W. J. M. Seviour

Department of Earth and Planetary Sciences, Johns Hopkins University, 3400 N. Charles St., Baltimore, MD 21218, USA

E-mail: wseviou1@jhu.edu

D. W. Waugh

Department of Earth and Planetary Sciences, Johns Hopkins University, 3400 N. Charles St., Baltimore, MD 21218, USA

L. M. Polvani

Lamont-Doherty Earth Observatory, Palisades, and Department of Applied Physics and Applied Mathematics, Columbia University, New York, New York, USA

G. J. P. Correa

Lamont-Doherty Earth Observatory, Columbia University, Palisades, New York, USA

model simulations; ranging from atmospheric models with prescribed ozone concentrations to coupled atmosphere-ocean models with interactive chemistry. Aside from models with interactive chemistry, the same change in ozone is prescribed in each simulation. A consistent poleward shift and intensification of the extratropical jet is found among simulations, although natural variability leads to large uncertainty in the magnitude of these responses. All models also simulate a widening of the southern edge of the Hadley cell, but its magnitude is less consistent. Consistency in the tropospheric response is improved further by normalizing by differences in the lower stratospheric temperature response to ozone depletion. Given this consistency among models, we propose that the majority of differences between model responses in previous studies has arisen from either statistical uncertainty due to natural variability, or differences in the prescribed ozone forcing.

Keywords ozone depletion · jet stream · Hadley cell

1 Introduction

Since the mid-1970s, significant trends in the Southern Hemisphere summertime atmospheric circulation have been observed. Most notably, the extratropical jet has shifted poleward by approximately 2° latitude and strengthened (Swart and Fyfe 2012; Hande et al 2012); a trend which is outside the range of natural variability found in the majority of coupled climate models (Thomas et al 2015). At the same time there has been a poleward expansion of the edge of the Hadley cell (Hu and Fu 2007; Seidel and Randel 2007; Davis and Rosenlof 2012), although there is large uncertainty in the rate of this expansion.

Several modeling studies have examined the roles of possible drivers of these trends, many of which have found stratospheric ozone depletion to be primarily responsible (Son et al 2010; Polvani et al 2011; Gerber and Son 2014; Waugh et al 2015; Schneider et al

2015). However, others have found a smaller response to ozone depletion and concluded that warming sea-surface temperatures (SSTs) play a larger role in driving these trends (Staten et al 2012; Quan et al 2014; Adam et al 2014). Gerber and Son (2014) quantified trends in the austral jet latitude and Hadley cell extent in simulations from the Coupled Model Intercomparison Projects phases 3 and 5 (CMIP3 and CMIP5) and the Chemistry-Climate Model Validation activity 2 (CCMVal2). They found some models to simulate almost no trend in the jet position over 1960-99, while others showed as much as a 5° poleward shift. They also found the CCMVal2 models to exhibit, on average, a stronger poleward shift than the CMIP3 or CMIP5 models, indicating that there may be systematic differences between different types of climate model. Kidston and Gerber (2010), Barnes and Hartmann (2010) and Garfinkel et al (2013) have also proposed that biases in the climatology and variability of climate models may be related to their sensitivity to external forcing. However, Simpson and Polvani (2016) have demonstrated that this relationship only exists in winter, so may have little impact on the response to ozone depletion (which is largest in summer).

There are two potential reasons for these differences in the modeled circulation response to ozone depletion: (a) differences in the ozone forcing (investigated by Waugh et al (2015) in the case of Hadley Cell trends), and (b) differences in the circulation response to a given ozone forcing. In this study, we aim to address the latter point; how robust is the modeled circulation response to a given ozone forcing? To do so, we analyze changes within 6 pairs of model simulations, representing conditions before and after significant ozone depletion, and each with the exact same change in ozone concentrations. In addition, we analyze 3 pairs of coupled chemistry model simulations. These models form a heirarchy, ranging from an atmospheric model, through to a coupled atmosphere-ocean model, and a coupled model with interactive chemistry.

2 Model Simulations

The pairs of simulations analyzed in this study along with their forcings are shown in Table 1. All simulations, except for those with interactive chemistry, use a zonal mean stratospheric ozone dataset developed by the International Global Atmospheric Chemistry (IGAC) and Stratosphere-troposphere processes and their Role in Climate (SPARC) activities (Cionni et al 2011), which we here refer to as the SPARC ozone dataset. This dataset was used in about half the models included in CMIP5. One simulation of each pair takes ozone concentrations from 1960, before significant ozone depletion, and the other from the year 2000.

The first two pairs of simulations (CAM-2000 and CAM-1960), which use the Community Atmospheric Model version 3 (CAM3) (Collins et al 2006), are extended versions of simulations previously analyzed by Polvani et al (2011) (their simulations were 50 years long rather than 100). These are atmosphere-only simulations with a horizontal resolution of T42 (roughly equivalent to a $2.8^\circ \times 2.8^\circ$ grid), and 26 hybrid vertical levels. Both simulations use sea ice concentrations and SST from the Hadley Centre sea ice and sea surface temperature (HadISST) data set (Rayner et al 2003). CAM-2000 uses a climatological annual cycle of SST and sea ice calculated from the years 1992-2008, while CAM-1960 uses a climatology from 1952-1968. Additionally CAM-2000 and CAM-1960 use greenhouse gas (GHG) concentrations for the years 2000 and 1960 respectively from the Special Report on Emissions Scenarios (SRES) A1B scenario (Nakicenovic et al 2000). In order to further test the sensitivity of the response to ozone depletion upon the background SST and GHG concentrations two further 50-year simulations have been performed with the CAM3 model: CAM-1870 and CAM-1870CM2. These both include pre-industrial (1870) GHG concentrations and SST; CAM-1870 takes its SST from the HadISST dataset at the year 1870, while

CAM-1870CM2 uses SSTs from a pre-industrial control simulation of the CM2.1 coupled model (Delworth et al 2006).

The two pairs of simulations GFDL-A and GFDL-O are from the Geophysical Fluid Dynamics Laboratory (GFDL) Earth System Model with Modular Ocean Model (ESM2Mc) model (Gnanadesikan et al 2015), a coarse resolution version of GFDL ESM2M (Dunne et al 2012). The GFDL-A simulations are from an atmosphere-only version of ESM2Mc with annually-repeating SSTs and sea ice concentrations while GFDL-O uses a fully coupled model. The atmospheric model used in these simulations has a horizontal resolution of $3.875^\circ \times 3^\circ$ with 24 vertical levels, and the ocean model used in GFDL-O has a $3^\circ \times 1.5^\circ$ resolution with 28 vertical levels. In the GFDL-A simulations, SST and sea ice concentrations are prescribed as the climatology of the 1960 ozone simulation of GFDL-O. Both GFDL-A and GFDL-O use preindustrial GHG concentrations, with a carbon dioxide concentration of 286 ppm, and simulations are run for 100 years.

In addition to the 6 pairs of time-slice simulations described above, we analyze 3 ensembles of transient simulations of models which include interactive chemistry. This means that they are able to predict stratospheric ozone concentrations based upon specified mixing ratios of chlorofluorocarbons and other ozone depleting substances (ODSs). In each case, we study differences between two 16-year periods–1960-1975 and 1995-2010–which are chosen to give similar ozone changes as the time-slice simulations.

We analyze two sets of simulations using the Goddard Earth Observing System Chemistry-Climate model (GEOSCCM) (Pawson et al 2008; Oman and Douglass 2014). The first three-member ensemble, GEOSCCM-A, is an atmosphere-only model (hoirzontal resolution $2^\circ \times 2.5^\circ$, 72 vertical levels) with sea ice and SST prescribed from the HadISST dataset from 1960-2006, and from the Reynolds dataset (Reynolds et al 2002) after 2006. The second four-member ensemble, GEOSCCM-O (simulations described in Li et al (2016)), cou-

ples the same atmospheric and chemistry model to the Modular Ocean Model version 4p1 (Griffies et al 2009). These GEOSCCM simulations are full historical simulations, and it is therefore important to note that it is not just ozone concentrations that change between the two selected periods, but GHG, volcanic, solar, and aerosol forcing also varies.

The Canadian Middle Atmosphere Model (CMAM) simulations were previously described by McLandress et al (2010), and use a coupled atmosphere-ocean model with comprehensive stratospheric chemistry. These simulations use a T31 horizontal resolution (roughly equivalent to a $6^\circ \times 6^\circ$ grid, with 71 verical levels. They use fixed 1960 GHG concentrations, aerosol, and solar forcing, but time-varying ODSs (specifically, this is the SCN2b scenario, described by Eyring et al (2008)).

3 Results

3.1 Response to ozone depletion

The effect of ozone depletion on zonal-mean temperature and wind is illustrated in Figure 1. This shows differences (2000 ozone minus 1960 ozone) for the CAM-2000 pair of simulations. A strong cooling is seen in the austral polar lower stratosphere (Figure 1(a)) and is largest during the spring, at the time of maximum ozone depletion. For the remainder of this study, we use the polar cap (60°-90°S), 100 hPa temperature averaged from October to Janurary (ONDJ), T_{polar}, as an index of the impact of ozone depletion on the stratosphere. This stratospheric cooling causes an intensification of the westerly winds in the polar stratosphere (Figure 1(b)), and a poleward shift and intensification of the tropospheric extratropical jet. Thompson and Solomon (2002) found the largest trends in the tropospheric jet to occur summer, so we use the mean tropospheric jet position and strength averaged from December to Janurary (DJF). In order to account for the relatively coarse resolution of some models, the

jet latitude, ϕ_{jet}, is determined as the location of the maximum of a quadratic fitted to the 850 hPa zonal-mean zonal wind at its maximum grid point and the two points either side. $\overline{u}_{\text{jet}}$ is then the value of this quadratic at this jet latitude. Visual inspection shows that a quadratic polynomial provides a good fit to the zonal-mean zonal wind for all simulations. The edge of the Southern Hemisphere branch of the Hadley cell, ϕ_{HC} is calculated as the position where the DJF meridional mass streamfunction at 500 hPa first crosses zero south of the tropical maximum. To again account for differences in model resolution, this zero-crossing latitude is determined through linear interpolation.

Figure 1(c) shows the relationship between ϕ_{jet} and T_{polar} for the CAM-2000 simulations. Each point represents a single year for each simulation. A clear cooling of the polar stratosphere and poleward shift of the tropospheric jet is seen in the 2000 ozone simulation relative to 1960 ozone. There is also large interannual variability in both simulations. In order to summarize the variability and correlation of ϕ_{jet} and T_{polar}, we also show ellipses representing the one standard deviation iso-contour of a 2 dimensional Gaussian distribution to which they are fitted.

The relationships between T_{polar}, and ϕ_{jet}, $\overline{u}_{\text{jet}}$, and ϕ_{HC} for each pair of simulations are shown in Figure 2. There are a wide range of climatological, pre-ozone depletion values of these parameters; ϕ_{jet} varies by about 12° latitude among models, ϕ_{HC} by about 10° latitude, $\overline{u}_{\text{jet}}$ by almost 3.5 m s^{-1}, and T_{polar} by about 8 K. The coupled chemistry models are consistent outliers in their climatology, with the GEOSCCM models having the most poleward extratropical jet and Hadley cell edge, and CMAM having the most equatorward. Note that the observed SH jet latitude is near 52°S (Swart and Fyfe 2012), indicating that the majority of models (except GEOSCCM) have an equatorward bias. This is consistent with Wilcox et al (2012) and Bracegirdle et al (2013), who find an equatorward bias in most of the CMIP5 models. However, in contrast to Bracegirdle et al (2013), we do not

find a reduced equatorward bias in atmosphere-only relative to coupled versions of the same model; indeed, for both the GEOSCCM and GFDL the coupled model has a more poleward jet (although this difference is small for the latter). Differences between model climatologies are significantly larger than the interannual variability (shown by the size of the ellipses). The effect of ozone depletion is broadly consistent across the models; the polar stratosphere is seen to cool, the extratropical jet shift polewards and strengthen. The Hadley cell also expands polewards, although by less than the extratropical jet.

Figure 3 summarizes these changes in the jet latitude and strength, and the Hadley cell extent resulting from ozone depletion in each of the simulation pairs. The horizontal bars represent the 95% uncertainty range for each difference, which is calculated by a bootstrap method. Individual years from each simulation are randomly resampled with replacement 10^4 times and then averaged to produce a distribution of average values for each simulation. Differences are then taken to between these averages to produce a distribution of differences. The uncertainty range for the difference is then that from the 2.5 to 97.5 percentiles of this distribution. These uncertainty ranges are a significant fraction of the response size for each variable. For example, even though the GFDL-O pair are two 100-year-long time-slice simulations, the uncertainty is approximately 17% of the response for $\Delta T_{\mathrm{polar}}$, 53% for $\Delta \phi_{\mathrm{jet}}$, 67% for $\Delta \overline{u}_{\mathrm{jet}}$, and about twice the response for $\Delta \phi_{\mathrm{HC}}$. This highlights the large interannual variability present in these models.

The responses to ozone depletion are broadly consistent across simulations, particularly when taking account of the uncertainty in the response in each simulation. Most consistent is $\Delta \phi_{\mathrm{jet}}$, showing a poleward shift near 1.3° latitude for every model with the exception of GEOSCCM-A. The value of $\Delta \phi_{\mathrm{jet}}$ for CAM-2000 (about 1.3°) is lower than that found by Polvani et al (2011) (1.9°). On closer inspection we find the difference to be larger over the first 50 years of these simulations (1.7°), the period analyzed by Polvani et al (2011)),

than the second 50 years (0.9°). This therefore explains most of the difference with Polvani et al (2011), and highlights the large variability present in these simulations (The 1.7° value is still slightly less than the 1.9° found by Polvani et al (2011), but this is likely due to methodological differences in the calculation of the jet latitude).

In order to isolate the tropospheric response to a given lower stratospheric perturbation, we normalize the tropospheric responses by ΔT_{polar}, shown in Figures 3(d,f,h). Following this normalization, the jet shift for GEOSCCM-A lies closer to the multi-model mean. This outlier can, therefore, be largely attributed to an anomalously strong stratospheric cooling, in turn resulting from a larger ozone depletion than other simulations.

When normalizing $\Delta\phi_{\text{jet}}$ by the stratospheric response, ΔT_{polar}, we find a fairly consistent value near $0.2°\text{K}^{-1}$. This value falls within the uncertainty range of the regression coefficients found by Gerber and Son (2014) for the relationship between polar stratospheric temperatures and the jet latitude in historical and future CMIP3, CMIP5, and CCMVal-2 simulations (see their Figure 3). In contrast to $\Delta\phi_{\text{jet}}$, normalizing $\overline{u}_{\text{jet}}$ by ΔT_{polar} does not improve the agreement between models, indicating that these differences may have other contributing factors besides the stratospheric temperature response. The average value of $\Delta\phi_{\text{HC}}$ is about a 0.6° poleward shift, approximately half that of $\Delta\phi_{\text{jet}}$, consistent with the 1:2 ratio reported by Kang and Polvani (2011) (because of the small sample size, the correlation of $\Delta\phi_{\text{HC}}$ and $\Delta\phi_{\text{jet}}$ for individual models is not statistically significant). Importantly, there do not appear to be any consistent differences between different types of model for any of the metrics analyzed. For instance, GFDL-A and GFDL-O give very similar responses. The different background SST and GHG concentrations in the CAM simulations also make little difference to their responses.

Kidston and Gerber (2010) and Barnes and Hartmann (2010) suggested that biases in the climatology of climate models (such as the jet latitude) may be linked to their sensi-

tivity to external forcing. In Figure 4 we test this relationship for our models, plotting the climatological average jet latitude, $< \phi_{\text{jet}} >$, against the jet shift, $\Delta\phi_{\text{jet}}$, for each pair of simulations. It can be seen that there is little relationship between these two parameters, and indeed, there is not a statistically significant correlation. This even applies for similar model types; for instance GEOSCCM-O and GEOSCCM-A have a similar climatological jet position, but GEOSCCM-A has the largest jet shift of all models, while GEOSCCM-O has the second weakest. This result supports the findings of Simpson and Polvani (2016), that the jet position/jet shift relationship only exists in winter.

3.2 Interannual variability

From Figure 1(c) it appears that ϕ_{jet} and T_{polar} are not correlated interannually, although they are clearly related under the influence of ozone depletion. This observation was made by Polvani et al (2011), who proposed that ϕ_{jet} and T_{polar} did not appear sufficiently correlated on interannual time scales in order to explain the long-term shift under ozone depletion, so that different mechanisms may be acting on short and long time scales.

To examine this we compare the interannual linear regression coefficient of ϕ_{jet} and T_{polar} for each simulation with the ratio of $\Delta\phi_{\text{jet}}$ to ΔT_{polar} for each pair. This is shown in Figure 5, where the red and blue bars show the interannual linear regression coefficient for the 1960 and 2000 simulations, respectively, and the black bar is the ratio of $\Delta\phi_{\text{jet}}$ to ΔT_{polar}, as in Figure 3(d) (In all cases the horizontal line represents the 95% uncertainty range.) For nearly every pair of simulations the interannual regression is consistent with the ozone depletion-induced change, indicating that the same mechanisms are acting on inter annual and longer time scales. An exception is GFDL-O where the interannual correlation appears larger than the ozone depletion-induced change, suggesting that in this model a

factor causing the correlation on interannual time scales may not act on longer time scales. However, this is a clear outlier.

To show how appearance of a small interannual correlation relative to the ozone depletion-induced change (e.g. Figure 1(c)) may come about we use a simple linear model of the dependence of ϕ_{jet} on T_{polar}, given by

$$\phi_{\text{jet}} = a + b(T_{\text{polar}} - T_0) + cN(0,1)\,, \tag{1}$$

where a, b, c and T_0 are constants, and $N(0,1)$ represents Guassian noise with mean 0 and variance 1. Figure 6 shows the relationship between ϕ_{jet} and T_{polar} for $a = -49^\circ$, $b = 0.2^\circ\text{K}^{-1}$ (the multi-model mean value of $\Delta\phi_{\text{jet}}/\Delta T_{\text{polar}}$), and $c = 1^\circ$. The blue and red points are generated identically, except for value of T_0 (205 K for the blue and 213 K for the red). These parameters have been chosen to give a similar appearance as Figure 1(c). By construction, the 'interannual' regression for both blue and red points is the same (with a value of b), and equal to the regression of the 'long term' shift between the two clouds of points (indicated by the black line). However, as with Figure 1(c), on first inspection ϕ_{jet} and T_{polar} do not appear correlated.

4 Conclusions

In this study we have examined the tropospheric response to stratospheric ozone depletion in a range climate model simulations. We have analyzed 6 pairs of simulations, each representing conditions before and after significant ozone depletion and each with the exact same change in ozone concentrations. In addition, we analyzed 3 pairs of coupled chemistry model simulations. These models form a heirarchy, ranging from an atmospheric model, through to a coupled atmosphere-ocean model, and a coupled model with interactive chemistry. We find that the poleward shift in the jet latitude is consistent among models. The

intensification of the jet and poleward expansion of the Hadley cell are less consistent, but interannual variability leads to a large degree of uncertainty in the changes, even within 100 year long simulations.

Consistent with Simpson and Polvani (2016), we here find no significant correlation between the climatological jet latitude and the ozone depletion-induced summertime jet shift, even though our model climatologies span about 12° latitude (which is about an order of magnitude greater than the mean response to ozone depletion). We also do not find any significant differences between different types of models, such as coupled and atmosphere-only models, or models with different prescribed SSTs or GHG concentrations. We find $\Delta\phi_{\text{jet}}/\Delta T_{\text{polar}} \approx 0.2\,^{\circ}\text{K}^{-1}$ to be consistent across models, as well as with the regression coefficients found by Gerber and Son (2014).

Given this apparent robust response, how can we explain the large differences in the jet response to ozone depletion found in CMIP3, CMIP5 and CCMVal-2 models (Gerber and Son 2014) (jet shift values ranging from almost no trend to a 5° poleward shift over 1960-99)? It is apparent from Figure 3 that despite considering differences from long (50 or 100 year) time slice simulations in this study, significant uncertainties in the jet responses remain, which are in some cases as large as the response itself. This can be attributed to the large interannual variability in the extratropical jet. Many of the historical and future simulations analyzed by Gerber and Son (2014) consisted of just a single ensemble member, and would therefore be subject to even larger uncertainties. Although Gerber and Son (2014) did not explicitly quantify uncertainties in individual model responses, it would be reasonable to suppose that a significant fraction of inter-model differences could be attributed to this effect of interannual variability. This highlights the importance of either large ensemble sizes or long time slice simulations in order to accurately quantify dynamical responses to an imposed forcing.

Acknowledgements We thank Luke Oman and Feng Li (NASA GSFC) for performing the GEOSCCM simulations. This work was funded by a Frontiers of Earth System Dynamics grant (FESD-1338814) from the US National Science Foundation.

References

Adam O, Schneider T, Harnik N (2014) Role of Changes in Mean Temperatures versus Temperature Gradients in the Recent Widening of the Hadley Circulation. J Climate 27:7450–7461, DOI 10.1175/JCLI-D-14-00140.1

Barnes EA, Hartmann DL (2010) Testing a theory for the effect of latitude on the persistence of eddy-driven jets using CMIP3 simulations. Geophys Res Lett 37:L15,801, DOI 10.1029/2010GL044144

Bracegirdle TJ, Shuckburgh E, Sallee JB, Wang Z, Meijers AJS, Bruneau N, Phillips T, Wilcox LJ (2013) Assessment of surface winds over the Atlantic, Indian, and Pacific Ocean sectors of the Southern Ocean in CMIP5 models: Historical bias, forcing response, and state dependence. J Geophys Res Atmos 118(2):547–562, DOI 10.1002/jgrd.50153

Cionni I, Eyring V, Lamarque JF, Randel WJ, Stevenson DS, Wu F, Bodeker GE, Shepherd TG, Shindell DT, Waugh DW (2011) Ozone database in support of CMIP5 simulations: results and corresponding radiative forcing. Atmos Chem Phys 11:11,267–11,292, DOI 10.5194/acp-11-11267-2011

Collins WD, Bitz CM, Blackmon ML, Bonan GB, Bretherton CS, Carton Ja, Chang P, Doney SC, Hack JJ, Henderson TB, Kiehl JT, Large WG, McKenna DS, Santer BD, Smith RD (2006) The Community Climate System Model version 3 (CCSM3). J Climate 19:2122–2143, DOI 10.1175/JCLI-D-11-00290.1

Davis SM, Rosenlof KH (2012) A multidiagnostic intercomparison of tropical-width time series using reanalyses and satellite observations. J Climate 25:1061–1078, DOI 10.1175/JCLI-D-11-00127.1

Delworth TL, Broccoli AJ, Rosati A, Stouffer RJ, Balaji V, Beesley Ja, Cooke WF, Dixon KW, Dunne J, Dunne Ka, Durachta JW, Findell KL, Ginoux P, Gnanadesikan A, Gordon CT, Griffies SM, Gudgel R, Harrison MJ, Held IM, Hemler RS, Horowitz LW, Klein Sa, Knutson TR, Kushner PJ, Langenhorst AR, Lee HC, Lin SJ, Lu J, Malyshev SL, Milly PCD, Ramaswamy V, Russell J, Schwarzkopf MD, Shevliakova E, Sirutis JJ, Spelman MJ, Stern WF, Winton M, Wittenberg AT, Wyman B, Zeng F, Zhang R (2006) GFDL's CM2 global coupled climate models. Part I: Formulation and simulation characteristics. J Climate 19:643–674, DOI 10.1175/JCLI3629.1

303 Dunne JP, John JG, Adcroft AJ, Griffies SM, Hallberg RW, Shevliakova S, Stouffer RJ, Cooke W, Dunne Ka,
304 Harrison, Matthew JKrasting JP, Malyshev SL, Milly PCD, Phillips PJ, Sentman LT, Samuels BL, Spel-
305 man MJ, Winton M, Wittenberg AT, Zadeh N (2012) GFDL's ESM2 Global Coupled Climate-Carbon
306 Earth System Models. Part I: Physical Formulation and Baseline Simulation Characteristics. J Climate
307 25:6646–6665, DOI 10.1175/JCLI-D-11-00560.1
308 Eyring V, Chipperfield MP, Giorgetta MA, Kinnison DE, Manzini E, Matthes K, Newman PA, Pawson S,
309 Shepherd TG, Waugh DW (2008) Overview of the New CCMVal Reference and Sensitivity Simulations
310 in Support of Upcoming Ozone and Climate Assessments and the Planned SPARC CCMVal Report.
311 SPARC Newsl No. 30:Stratospheric Processes and their Role in Climate,
312 Garfinkel CI, Waugh DW, Gerber EP (2013) The effect of tropospheric jet latitude on coupling between
313 the stratospheric polar vortex and the troposphere. J Climate 26:2077–2095, DOI 10.1175/JCLI-D-12-
314 00301.1
315 Gerber EP, Son SW (2014) Quantifying the Summertime Response of the Austral Jet Stream and Hadley
316 Cell to Stratospheric Ozone and Greenhouse Gases. J Climate 27:5538–5559, DOI 10.1175/JCLI-D-13-
317 00539.1
318 Gnanadesikan A, Pradal MA, Abernathey R (2015) Isopycnal mixing by mesoscale eddies signif-
319 icantly impacts oceanic anthropogenic carbon uptake. Geophys Res Lett 42:4249–4255, DOI
320 10.1002/2015GL064100
321 Griffies SM, Schmidt M, Herzfeld M (2009) Elements of mom4p1. GFDL Ocean Gr Tech Rep DOI
322 10.1002/047174882X, ISBN 0-471-06259-6
323 Hande LB, Siems ST, Manton MJ (2012) Observed Trends in Wind Speed over the Southern Ocean. Geophys
324 Res Lett 39:L11,802, DOI 10.1029/2012GL051734
325 Hu Y, Fu Q (2007) Observed poleward expansion of the Hadley circulation since 1979. Atmos Chem Phys
326 Discuss 7:9367–9384, DOI 10.5194/acpd-7-9367-2007
327 Kang SM, Polvani LM (2011) The interannual relationship between the latitude of the eddy-driven jet and
328 the edge of the Hadley cell. J Climate 24(2):563–568, DOI 10.1175/2010JCLI4077.1
329 Kidston J, Gerber EP (2010) Intermodel variability of the poleward shift of the austral jet stream in the
330 CMIP3 integrations linked to biases in 20th century climatology. Geophys Res Lett 37:L09,708, DOI
331 10.1029/2010GL042873

Li F, Vikhliaev YV, Newman PA, Pawson S, Perlwitz J, Waugh DW, Douglass AR (2016) Impacts of Interactive Stratospheric Chemistry on Antarctic and Southern Ocean Climate Change in the Goddard Earth Observing System - Version 5 (GEOS-5). J Climate 29:3199–3218, DOI 10.1175/JCLI-D-15-0572.1

McLandress C, Jonsson AI, Plummer DA, Reader MC, Scinocca JF, Shepherd TG (2010) Separating the Dynamical Effects of Climate Change and Ozone Depletion. Part I: Southern Hemisphere Stratosphere. J Climate 23:5002–5020, DOI 10.1175/2010JCLI3586.1

Nakicenovic N, Alcamo J, Davis G, de Vries B, Fenhann J, Gaffin S, Gregory K, Grubler A, Jung TY, Kram T, Lebre La Rovere E, Michaelis L, Mori S, Morita T, Pepper W, Pitcher H, Price L, Riahi K, Roehrl A, Rogner HH, Sankovski A, Schlesinger M, Shukla P, Smith S, Swart R, van Rooijen S, Victor N, Dadi Z (2000) Special Report on Emissions Scenarios: A Special Report of Working Group III of the Intergovernmental Panel on Climate Change. Tech. rep., Cambridge University Press

Oman LD, Douglass AR (2014) Improvements in total column ozone in GEOSCCM and comparisons with a new ozone-depleting substances scenario. J Geophys Res 119:5613–5624, DOI 10.1002/2014JD021590

Pawson S, Stolarski RS, Douglass AR, Newman PA, Nielsen JE, Frith SM, Gupta ML (2008) Goddard earth observing system chemistry-climate model simulations of stratospheric ozone-temperature coupling between 1950 and 2005. J Geophys Res Atmos 113:D12,103, DOI 10.1029/2007JD009511

Polvani LM, Waugh DW, Correa GJP, Son SW (2011) Stratospheric Ozone Depletion: The Main Driver of Twentieth-Century Atmospheric Circulation Changes in the Southern Hemisphere. J Climate 24:795–812, DOI 10.1175/2010JCLI3772.1

Quan XW, Hoerling MP, Perlwitz J, Diaz HF, Xu T (2014) How Fast Are the Tropics Expanding? J Clim 27:1999–2013, DOI 10.1175/JCLI-D-13-00287.1

Rayner NA, Parker DE, Horton EB, Folland CK, Alexander LV, Rowell DP, Kent EC, Kaplan A (2003) Global analyses of sea surface temperature, sea ice, and night marine air temperature since the late nineteenth century. J Geophys Res 108:D14,4407, DOI 10.1029/2002JD002670

Reynolds RW, Rayner NA, Smith TM, Stokes DC, Wang W (2002) An improved in situ and satellite SST analysis for climate. J Climate 15:1609–1625

Schneider DP, Deser C, Fan T (2015) Comparing the impacts of tropical SST variability and polar stratospheric ozone loss on the Southern Ocean westerly winds. J Climate 28:9350–9372, DOI 10.1175/JCLI-D-15-0090.1

Seidel DJ, Randel WJ (2007) Recent widening of the tropical belt: Evidence from tropopause observations. J Geophys Res 112:D20,113, DOI 10.1029/2007JD008861

Simpson IR, Polvani LM (2016) Revisiting the relationship between jet position, forced response, and annular mode variability in the southern mid-latitudes. Geophys Res Lett 43:1–8, DOI 10.1002/2016GL067989

Son SW, Gerber EP, Perlwitz J, Polvani LM, Gillett NP, Seo KH, Eyring V, Shepherd TG, Waugh D, Akiyoshi H, Austin J, Baumgaertner A, Bekki S, Braesicke P, Brühl C, Butchart N, Chipperfield MP, Cugnet D, Dameris M, Dhomse S, Frith S, Garny H, Garcia R, Hardiman SC, Jöckel P, Lamarque JF, Mancini E, Marchand M, Michou M, Nakamura T, Morgenstern O, Pitari G, Plummer DA, Pyle J, Rozanov E, Scinocca JF, Shibata K, Smale D, Teyssèdre H, Tian W, Yamashita Y (2010) Impact of stratospheric ozone on Southern Hemisphere circulation change: A multimodel assessment. J Geophys Res 115:D00M07, DOI 10.1029/2010JD014271

Staten PW, Rutz JJ, Reichler T, Lu J (2012) Breaking down the tropospheric circulation response by forcing. Clim Dyn 39:2361–2375, DOI 10.1007/s00382-011-1267-y

Swart NC, Fyfe JC (2012) Observed and simulated changes in the Southern Hemisphere surface westerly wind-stress. Geophys Res Lett 39:6–11, DOI 10.1029/2012GL052810

Thomas JL, Waugh D, Gnanadesikan A (2015) Decadal variability in the Southern Hemisphere extratopical circulation: Recent trends and natural variability. Geophys Res Lett 42:5508–5515, DOI 10.1002/2015GL064521

Thompson DWJ, Solomon S (2002) Interpretation of recent Southern Hemisphere Climate Change. Science 296:895–899, DOI 10.1126/science.1069270

Waugh DW, Garfinkel CI, Polvani LM (2015) Drivers of the Recent Tropical Expansion in the Southern Hemisphere: Changing SSTs or Ozone Depletion? J Clim 28:6581–6586, DOI 10.1175/JCLI-D-15-0138.1

Wilcox LJ, Charlton-Perez AJ, Gray LJ (2012) Trends in Austral jet position in ensembles of high- and low-top CMIP5 models. J Geophys Res Atmos 117:1–10, DOI 10.1029/2012JD017597

Table 1 Model integrations analyzed in this study and their forcings

Pair name	Model	Ozone	GHG	SST	Length
CAM-2000	CAM3	SPARC (1960/2000)	2000 (SRES-A1b)	HadISST (2000)	100 years
CAM-1960	CAM3	SPARC (1960/2000)	1960 (SRES-A1b)	HadISST (1960)	100 years
CAM-1870	CAM3	SPARC (1960/2000)	1870	HadISST(1870)	50 years
CAM-1870CM2	CAM3	SPARC (1960/2000)	1870	CM2.1 control	50 years
GFDL-A	ESM2Mc atmos	SPARC (1960/2000)	1860	ESM2Mc control	100 years
GFDL-O	ESM2Mc	SPARC (1960/2000)	1860	Coupled	100 years
GEOSCCM-A	GEOSCCM	Interactive chemistry	Transient	HadISST/Reynolds	3x16 years
GEOSCCM-O	GEOSCCM	Interactive chemistry	Transient	Coupled	4x16 years
CMAM	CMAM	Interactive chemistry	1960	Coupled	3x16 years

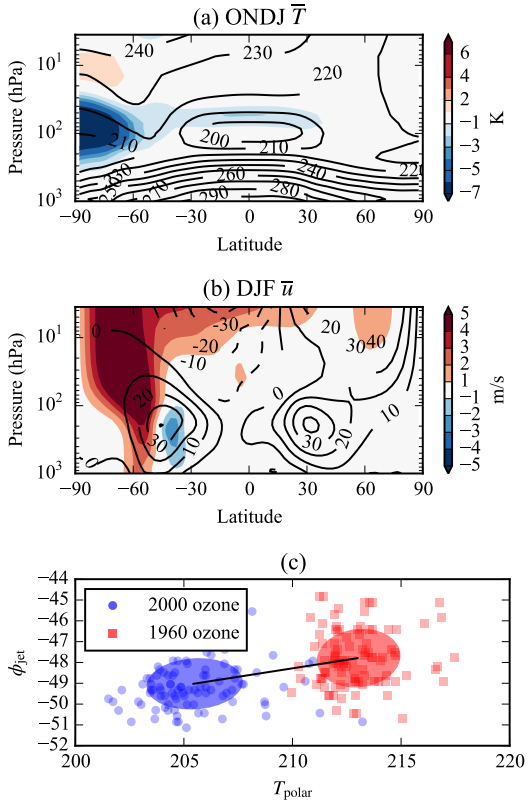

Fig. 1 ONDJ zonal-mean temperature (a) and DJF zonal-mean zonal wind (b) differences (colors) for the CAM-2000 simulations. Line contours represent the climatology for the 1960 ozone simulation. (c) Shows the co-variability of the DJF tropospheric jet latitude, ϕ_{jet} and ONDJ polar cap (65-90°S) temperature at 100 hPa, T_{polar}. Ellipses represent the one standard deviation iso-contour of a Guassian distribution to which the distributions are fitted.

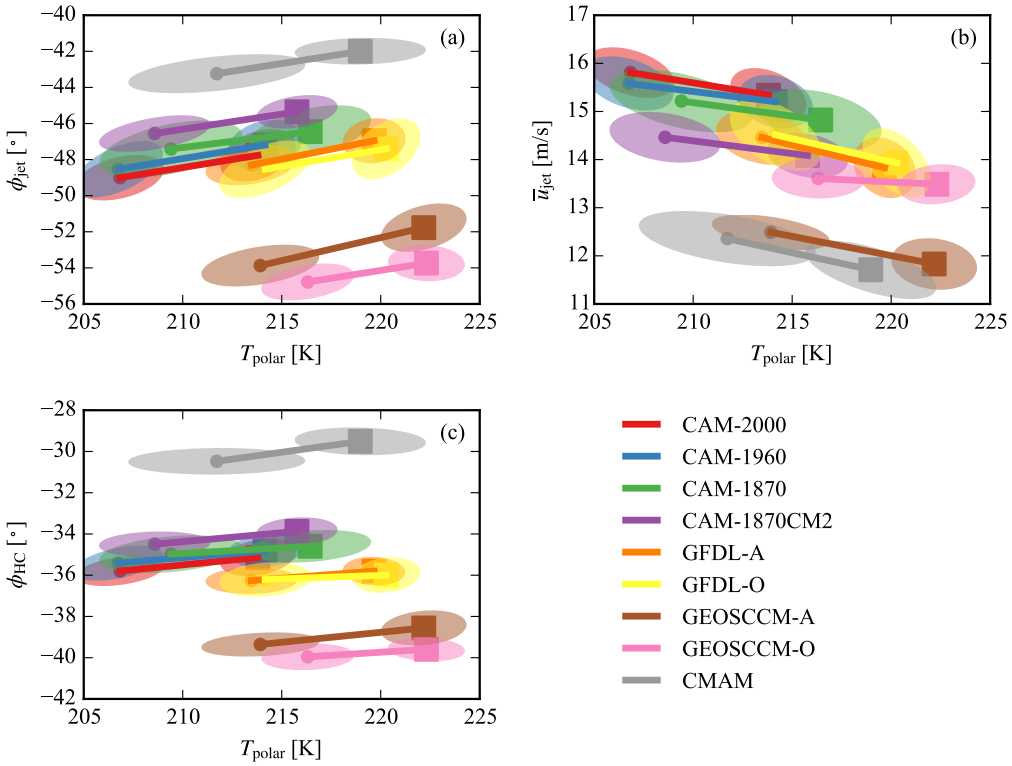

Fig. 2 Relation between ONDJ 100 hPa polar cap (65-90°S) temperature, T_{polar}, DJF average tropospheric jet latitude, ϕ_{jet} (a), jet strength, $\bar{u}_{\text{jet}}$ (b), and Hadley cell edge, ϕ_{HC} (c), for each of the model simulations. Squares represent simulations with year 1960 ozone, circles with 2000 ozone. Ellipses represent one standard deviation of interannual variability as in Figure 1.

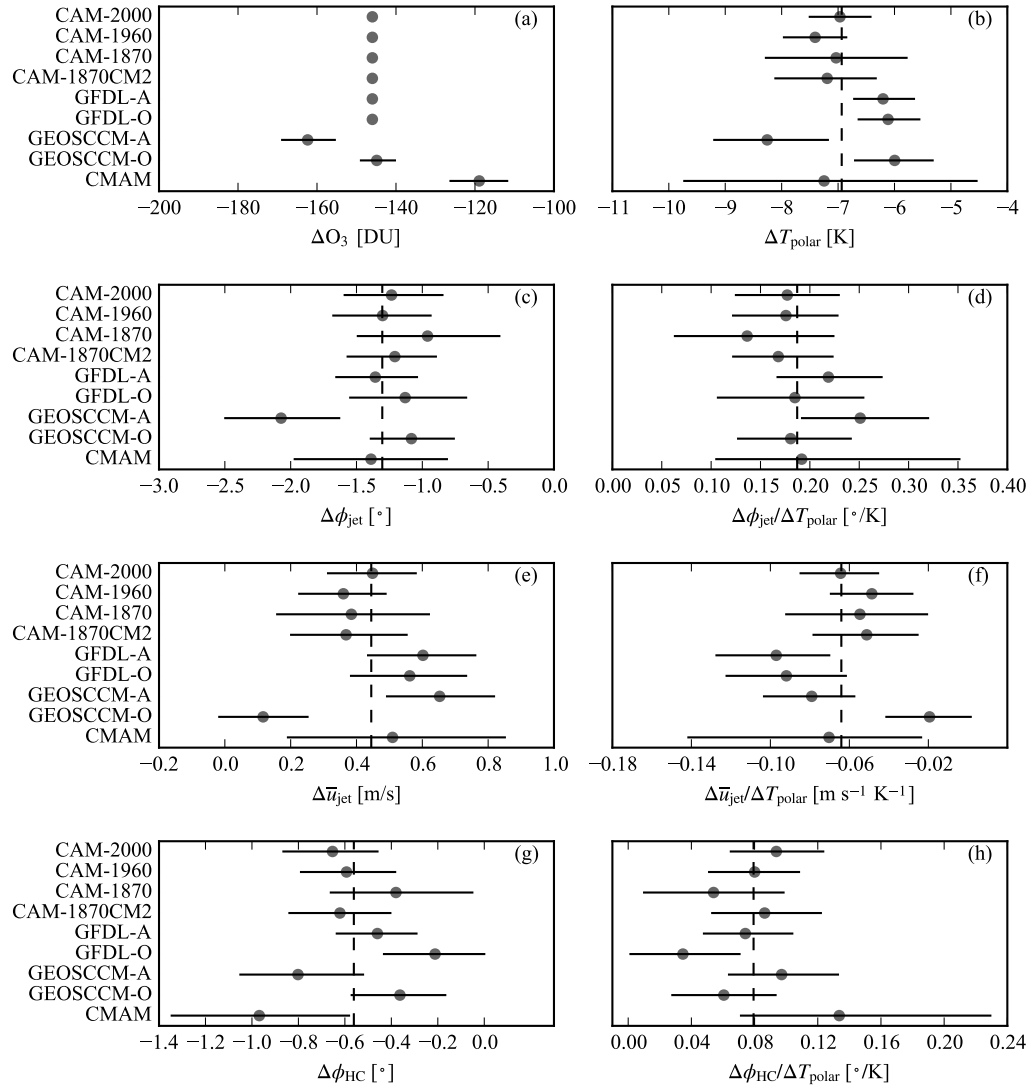

Fig. 3 Changes between simulations in October mean polar cap (60-90°S) column ozone, ΔO_3 (a), ONDJ mean 100 hPa polar cap temperature ΔT_{polar} (b), DJF tropospheric jet latitude, $\Delta\phi_{\text{jet}}$ (c), jet strengh $\Delta\overline{u}_{\text{jet}}$ (e), and Hadley cell edge $\Delta\phi_{\text{HC}}$ (g). (d,f,h) Show the corresponding tropospheric responses normalized by ΔT_{polar}. Horizontal bars represent the 95% uncertainty range, determined by a bootstrap test, and dashed vertical lines show the multi-model mean.

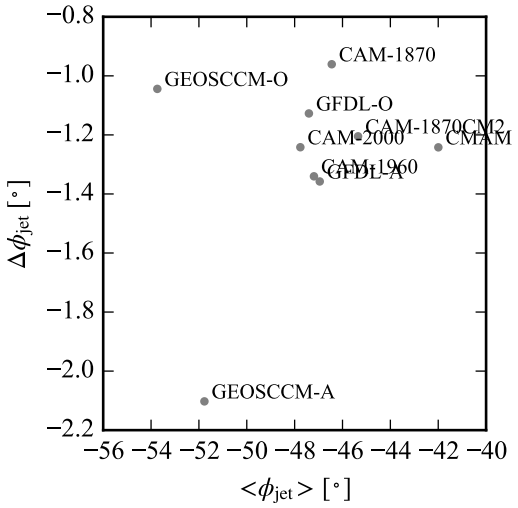

Fig. 4 Relationship between the mean DJF tropospheric jet latitude of the pre-ozone depletion simulation, $<\phi_{\rm jet}>$, and the jet shift under ozone depletion, $\Delta\phi_{\rm jet}$, for each of the simulations.

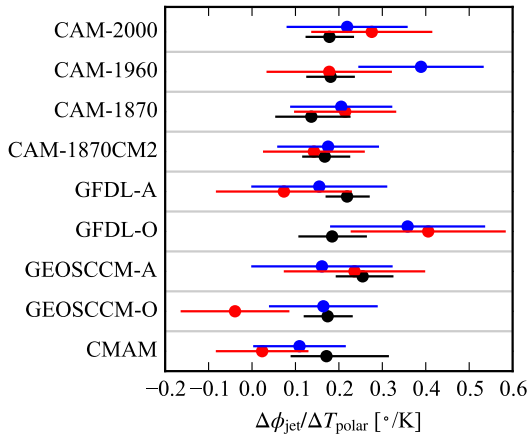

Fig. 5 Linear regression of interannual variability in jet latitude with 100 hPa polar cap temperature, for the 1960 ozone (red) and 2000 ozone (blue) simulations. Black dots inticate the slope between the means of the 1960 and 2000 ozone simulations (i.e. the values shown in Figure 3(d)). Horizontal bars represent the 95% uncertainty interval.

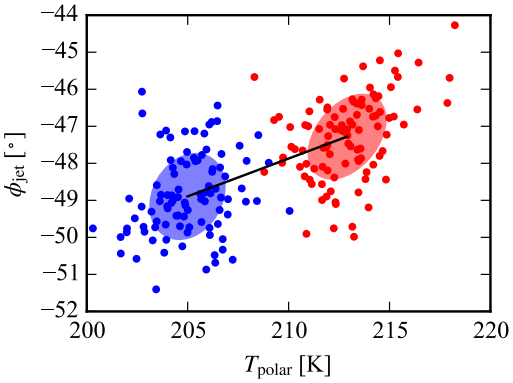

Fig. 6 Example of jet latitude and polar cap temperature generated using a simple linear relation given by equation 1. Ellipses are shown as in Figure 1(c).